POLYMER MICROROD ARRAYS PREPARED BY NON-DESTRUCTIVE MOLDING EVALUATED BY REAL SPACE IMAGE ANALYSIS

Reinald Hillebrand,[1] Silko Grimm,[1] Reiner Giesa,[2] Hans-Werner Schmidt,[2] Klaus Mathwig,[1] Ulrich Gösele[1] and Martin Steinhart [1]

[1]Max Planck Institute of Microstructure Physics, Weinberg 2, 06120 Halle, Germany
[2]Macromolecular Chemistry I and Bayreuth Institute for Macromolecular Research (BIMF), University of Bayreuth, 95440 Bayreuth, Germany

Introduction

Ensembles of aligned polymer nanorods and microrods are promising materials for self-cleaning surfaces[1], bioinspired adhesive structures[2], tissue engineering[3] or sensor arrays. Their production by means of porous templates such as self-ordered nanoporous anodic aluminum oxide (AAO)[4] or macroporous silicon[5], which contain ordered arrays of cylindrical pores, is well established.[6] The release of the rods commonly requires destruction of the templates in a wet-chemical etching step. Moreover, the occurrence of capillary forces during subsequent drying leads to agglomeration of the rods deteriorating the structural integrity of the arrays they constitute. Nondestructive mechanical extraction of microrods consisting of thermoplastics from thus recyclable macroporous silicon templates suffered from plastic deformation of the microrods.[7] However, mechanical lift-off of crosslinked polyacrylate rods showing elastic behavior at small deformations from macroporous silicon and AAO yields ordered rod arrays.[8] Digital microscopic images may contain information about array properties such as topography, mechanical properties, conductivity, polarization orientations etc., which are encoded by brightness. Real space image analysis of micrographs such as scanning electron microscopy (SEM) images allows evaluating the integrity of array structures and their spatial uniformity. Moreover, spatial fluctuations of the array properties can be quantified. Here we show that the relative height distributions of polymeric nanorods and microrods displayed in different SEM images can be compared by real space image analysis, and that the portion of fractured fibers can be determined.

Experimental

Materials. Macroporous silicon[5] (pore diameter: 1μm, lattice constant: 2μm, pore depth: 10μm) and self-ordered AAO[4] (pore diameter: 180nm, lattice constant: 500nm, pore length: 1μm) were produced according to procedures reported in the literature and used as molds for the preparation of the polymeric nanorods and microrods. The pores were closed at the bottom, and the porous layers were attached to underlying substrates, i.e., to silicon wafers in case of macroporous silicon and to aluminum discs in the case of AAO. The crosslinkable polyacrylate prepolymer PO 77F from the BASF Laromer® curing resin product line, or mixtures of PO 77F and tripropylene glycol diacrylate (PO 77F MX; mixing ratio 70:30), were used to infiltrate macroporous silicon or AAO. To render the pore walls, which have initially high surface energy, into surfaces with a low surface energy, we modified the templates by silanization prior to the infiltration. To this end, macroporous silicon was immersed for one hour in a boiling mixture of sulfuric acid and hydrogen peroxide (30:70). Then the templates were rinsed in water and ethanol and dried at room temperature. AAO was heated to 50°C in a hydrogen peroxide (30%) solution for 2 hours. Subsequently, the AAO was rinsed three times with water and dried at 120 °C for 15 minutes. The thus-treated templates were then heated to 90°C for 3 hours and to 130°C for another 3 hours, respectively, in presence of 0.05 ml of the hydrophobic silane 1H,1H,2H,2H perfluorodecyltrichlorosilan ($C_{10}H_4Cl_3F_{17}Si$, 97%, purchased from Aldrich). The silanization of the pore walls resulted in a decrease of the pore diameter by about 30nm. All chemicals were used without purification.

Preparation of the polyacrylate rod arrays. The polyacrylate prepolymer was infiltrated into the templates by a pressure impregnation technique and subsequently photocrosslinked with a Fusion UV Curing F 300 lamp (D lamp; 120W/cm). A doubleside adhesive tape was glued onto the underside of the templates and onto the polymer film covering the template surface. Then, the samples were mounted on a linear motion device with an attached load cell. First, a piston was pressed onto the sample at a rate of 0.2mm/min with a maximum compressive load of -40N. Then, the rods were extracted at a rate of 0.1 mm/min with a force of around 0.4 N.

Image analysis. Microrod arrays of the two model resins with a rod diameter of 1μm, a rod length of 10μm and a lattice constant of 2μm were mechanically extracted and imaged with a JEOL 7500F scanning electron microscope operated at low acceleration voltages. Several SEM images containing exemplary features were selected as examples in case for detailed numerical image analysis. The image analysis program *Image J* was used to identify single rods by a thresholding procedure that have brightness larger than their surrounding. The ordering of the array structures was analyzed by means of pair distribution functions (PDFs) and angular distribution functions (ADFs).[9]

Results and Discussion

Ordered microrod and nanorod arrays. The silanization of the pore walls resulted in the minimization of the adhesion between the polymer rods and the pore walls, therefore facilitating mechanical extraction of the arrays. **Figure 1a** shows a large field view of PO 77F nanorods extracted from AAO. The image reveals that the characteristic grain structure of the AAO was transferred to the rod array. In **figure 1b**, a large-field view of the AAO, which is still intact after the lift-off process, is shown.

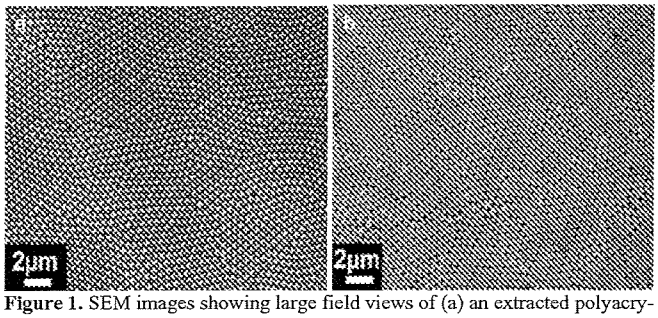

Figure 1. SEM images showing large field views of (a) an extracted polyacrylate nanorod array (diameter ≈ 120nm) and (b) the AAO template after extraction.

A cross-sectional view of the nanorod array (**Figure 2a**) confirms that the nanorods do not stick together. They show neither bending nor bunching. They possess a uniform diameter of approximately 120 nm and a height of 900 nm, respectively, corresponding to an aspect ratio of 7.5. Experiments with polyacrylate microrods extracted from macroporous silicon yield perfectly ordered microrod arrays (**Figure 2b**). Careful examination by SEM revealed that the extracted rods are uniform in diameter along their entire length. In contrast to microrods consisting of thermoplastic polymers[6] such as polystyrol, necking or yielding did not occur upon extraction.

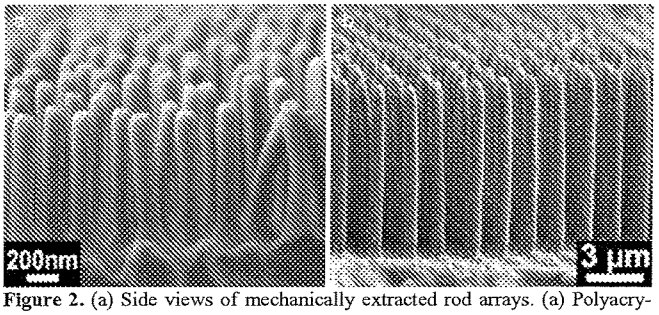

Figure 2. (a) Side views of mechanically extracted rod arrays. (a) Polyacrylate nanorods having a length of approximately 900nm; (b) polyacrylate microrods with an aspect ratio of 10.

Evaluation of microrod arrays by image processing. Figure 3a shows a top view, and **Figure 3b** a bird's eye view of microrod arrays extracted from macroporous silicon. The SEM pictures were taken in the lower secondary electron detection mode with an acceleration voltage of 2 keV. The top view image seen in **figure 3a** shows clearly the quadratic lattice of the array. The lattice constant of 2μm can be extracted from the corresponding pair distribution function displayed in **figure 3c**. The PDF exhibits two sharp peaks 2.0 μm and 2.8μm, corresponding to the nearest and second-nearest neighbor distance being expected for a quadratic lattice. Correspondingly, the ADF (**Figure 3d**) shows a sharp peak at the nearest neighbor angle of 90°. The

SEM image shown in **figure 3b** is characterized by a specimen tilt angel (combined with in-plane rotation). The corresponding PDF contains therefore a splitting of the nearest neighbor peak into two peaks at distances of 1.8 µm and 2.5 µm. The apparent distortion of the lattice leads also to splitting of the nearest neighbor angle peak in the ADF, were two new peaks at 82° and 98° appear. Nevertheless the corresponding distribution functions reveal an ordered arrangement which is quadratic.

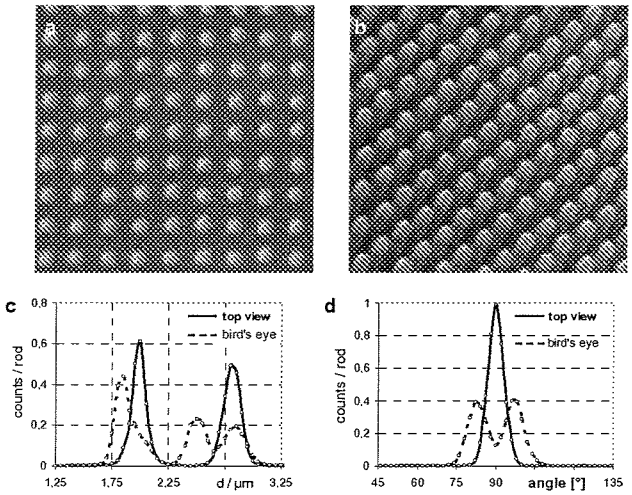

Figure 3. (a) SEM top view and (b) SEM bird's eye view of an ordered microrod array with a rod diameter of 1µm and a lattice constant of 2µm extracted from macroporous silicon; (c) PDFs and (d) ADFs extracted from the SEM images seen in (a) and (b).

Figure 4a shows a microrod array consisting of PO 77F microrods which was extracted from macroporous silicon. The rods are obviously intact, and only a small number of them broke. In contrast, an array of microrods consisting of PO 77FMX, a stiffer material than PO 77F, contains a large portion of microds fractured due to the impact of shear forces during the lift-off process (**Figure 4b**).

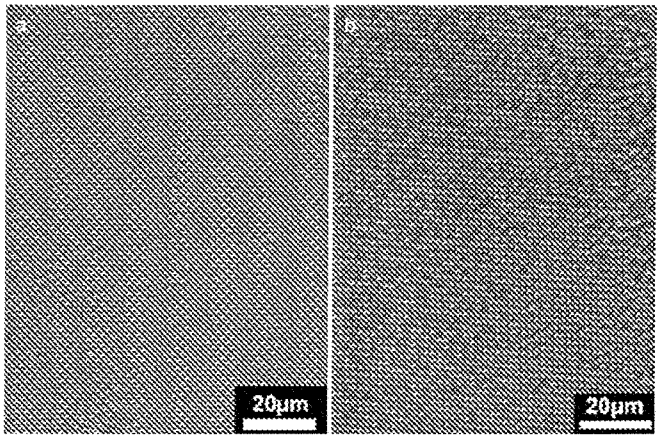

Figure 4. SEM images of (a) an array of microrods consisting of the polyacrylate PO 77F extracted from macroporous silicon and (b) of a PO 77F MX microrod array containing a large fraction of broken rods.

Carrying out consecutive thresholding procedures in which the threshold value *I_T* is successively shifted allows counting the rods identified for each threshold value and therefore deriving cumulative distribution functions of the relative rod lengths, which are correlated with the brightness of the tips of the rods. The resulting cumulative frequency distribution functions *N(I_T)* of the relative rod lengths, on which, however, contrast saturation effects superimpose, are shown in **figure 5**. In case of **figure 4a**, the high uniformity of the rod array is obvious from the plateau in the corresponding cumulative frequency distribution. Between *I_T* values of 110 and 190 of 255 intensity values, the number of identified rods is virtually constant, thus indicating that they are uniform in length.

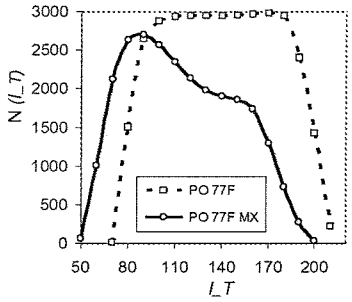

Figure 5. Cumulative frequency distribution of the relative rod lengths derived from the SEM images seen in **figure 4**.

However, the large portion of fractured rods seen in **figure 4b** is obvious from the monotonic decrease of the number of identified rods with increasing *I_T*, because broken and therefore shorter rods merge in the background. The portion of broken rods was calculated to be 32% by summing up the number of entities that vanish when *I_T* is increased from 90 to 160. The degree of self-similarity of normalized cumulative distribution functions can be used to quantitatively compare the uniformity of different arrays. To this end, the width at half maximum of the corresponding autocorrelation functions (ACFs) as well as the area under the ACFs can be used as quanitative measures.

Conclusions

In conclusion, we have demonstrated the nondestructive mechanical extraction of arrays of crosslinked polyacrylate nanorods and microrods from thus recyclable nanoporous AAO and macroporous silicon templates without necking, yielding or cohering. Furthermore, we have developed procedures based on real space image analysis of scanning electron microscopy images of the arrays thus released to determine the number of fractured rods and to quantify the uniformity of the array properties. The methods reported here may enable, on the one hand, high throughput production of functional nanorod and microrod arrays. On the other hand, real space image processing allows rapid monitoring of the array properties.

Acknowledgements. Technical support by K. Sklarek and S. Kallaus (MPI Halle) as well as by M Gietl (University of Bayreuth), funding by the German Research Foundation (Materials World Network, STE 1127/5 and SFB 481, project A6), and the donation of Laromer resins from BASF SE, Ludwigshafen, is gratefully acknowledged.

References

(1) Barthlott, W.; Neinhuis, C. *Planta*, **1997**, *202*, 1.
(2) Gao H., Wang X., Yao H., Gorb S. and Arzt E., *Mechanics of Materials*, **2005**, 37, 275-285.
(3) Li, W.-J.; Laurencin, C. T.; Caterson, E. J.; Tuan, R. S.; Ko, F. K., *J. Biomed. Mater. Res.*, 2002, 60, 613.
(4) Masuda, H.; Yada K.; Osaka, A., *Jpn. J. Appl. Phys. Part 2*, **1998**, *37*, L1340.
(5) Lehmann, V., *J. Electrochem. Soc.*, **1993**, *140*, 2836.
(6) Martin, C. R. *Science* **1994**, *266*, 1961.
(7) Grimm, S.; Schwirn, K.; Göring, P.; Knoll, H.; Miclea, P. T.; Greiner, A.; Wendorff, J. H.; Wehrspohn, R. B.; Gösele, U.; Steinhart, M., *Small*, **2007**, *3*, 993.
(8) Grimm S, Giesa R, Sklarek K, Langner A., Gösele U., Schmidt H-W., Steinhart M., *Nano Lett.*, **2008**, 8, 1954–1959.
(9) Hillebrand R., Müller F., Schwirn K., Lee W., Steinhart M., *ACS Nano* **2008**, *2*, 913-920.